Observation of a Plateau Electron Distribution Function Due to Electron Cyclotron Heating for an Efficient Plug Potential Formation

T. Cho, M. Hirata, K. Ogura,[a] E. Takahashi, T. Kondoh,[b] N. Yamaguchi, K. Masai,[c] K. Hayashi, I. Katanuma, K. Ishii, T. Saito, Y. Kiwamoto, K. Yatsu, and S. Miyoshi

Plasma Research Centre, University of Tsukuba, Ibaraki 305, Japan

(Received 27 November 1989)

A plateau-shaped electron distribution function is observed when an electrostatic electron-trapping potential is formed by the electron cyclotron heating (ECH) in the plug region of the GAMMA 10 tandem mirror. Also, a remarkable thermal-isolation effect due to a kV-range thermal barrier is observed along with a difference between distribution functions in thermally separated regions. These new findings as well as the relation between ion-confining potentials and thermal-barrier potentials in the kV range consistently support the validity of Cohen's strong ECH theory.

PACS numbers: 52.55.Pi, 52.50.Gj, 52.55.Jd, 52.70.La

Recent research related to electron cyclotron heating (ECH) has been intensified for several types of plasma confinement devices.[1-6] In tandem mirrors,[7] ECH is utilized for the formation of a thermal-barrier potential, ϕ_b,[8,9] in the barrier region, as well as of an ion-confining potential, ϕ_c, in the plug region. The enhancement of ϕ_c is theoretically predicted with increasing ϕ_b,[10-12] because of the efficient heating of localized plug electrons; they are thermally isolated from the large volume of central-cell electrons when ϕ_b is formed. The theoretical scaling of ϕ_c vs ϕ_b has been described in terms of Cohen's weak ECH[10] and strong ECH theories.[11] The scaling law of the potentials is one of the most important and critical items for the future development and the design of thermal-barrier tandem mirrors. However, its experimental studies compared with the theories have been limited to our preliminary results alone,[13] even in which only the relation between ϕ_c and ϕ_b was treated.

One of the most essential and direct methods to study the bases of these scaling theories[10-12] is to observe the plug electron distribution function, f_{ep}, since an essential difference of the strong ECH theory from the weak one is whether the characteristic time of plug electron heating by ECH for a plateau distribution formation[11] dominates over the collisions for a Maxwellian formation.[10]

In this Letter, we report (i) the first observation of the formation of a plateau electron distribution function in the plug using several x-ray diagnostics. (ii) In addition, our previous experiments merely suggested a transition tendency from the weak to the strong ECH scaling with increasing ϕ_b, since the two theories did not provide values with clear differences for the limited range of the ϕ_c vs ϕ_b data[13] (most data being at $\phi_b \leqq 0.7$ kV). Here, we report a wider range of data ($\phi_b \leqq 1.2$ kV), which show a clear discrepancy from the weak ECH scaling in the high-ϕ_b region. These potential data again support the strong ECH scaling as observed in (i) using the x-ray diagnostics. (iii) Furthermore, the first direct observation of the thermal-isolation effect[14] due to a kV-range thermal barrier is reported by showing a large difference in x-ray spectra between the central cell and the plug. These new findings give clear pictures of the thermal-isolation effect due to ϕ_b as well as of the plug electron heating process according to the strong ECH theory for a kV-range ϕ_c formation.

The experiments have been carried out in GAMMA 10,[8,12] which is a minimum-B anchored tandem mirror with outboard plug and barrier cells. It has an axial length $L=27$ m and the total volume of the vacuum vessel is 150 m^3. The central cell has $L=6$ m, a limiter diameter $d=36$ cm, and the magnetic-field intensity at the midplane $B=0.405$ T with a mirror ratio $R=5.2$. The plug and barrier cells are axisymmetric mirrors with $L=2.5$ m, $B=0.497$ T, and $R=6.2$. Microwaves (28 GHz and 140 kW) are injected as an extraordinary mode into the barrier (BECH) and the plug (PECH) regions, respectively.[8] Neutral-beam injections for a sloshing ion formation[7,8] and ion cyclotron heating (6.2 MHz and 200 kW) in the central cell are employed.[14]

The energy spectra, from x-ray pulse-height analyses (PHA), ranging from 0.7 to 150 keV in the plug are measured with a combination of a Si(Li) detector (a depletion layer $p=0.27$ cm with an 8-μm Be window) and a pure Ge detector ($p=1$ cm with a 0.125-mm Be window). X-ray tomographic reconstructions using microchannel plates (MCP) with fifty channels[15] are utilized for obtaining the x-ray radial profiles in the plug, barrier, and central-cell regions. Here, we use the detailed calibration data on the MCP[16-19] as a function of x-ray energy from 0.06 to 82 keV and incident angle; these have been investigated using synchrotron radiation for the precise x-ray data analyses. In order to estimate the electron distribution functions the x-ray absorption method[4,8] is employed using polypropylene, polyester, and aluminum absorbers. A plug electron-confining potential ϕ_{pb} ($=\phi_c+\phi_b$) is measured with multigrided electrostatic end-loss-ion energy analyzers (ELA's)[13] and an **E**$\|$**B** end-loss-ion spectrometer (ELIS) from the

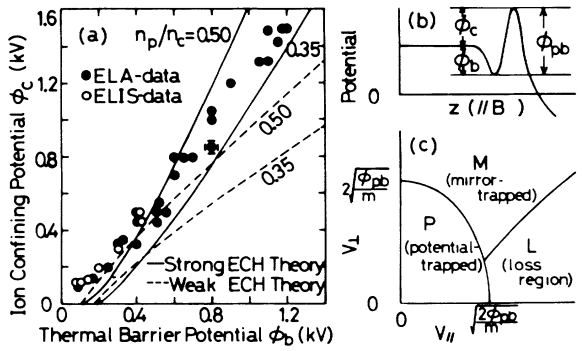

FIG. 1. (a) Scaling data on ϕ_c vs ϕ_b as compared with the ECH theories. (b) An axial potential profile. (c) A model of an electron velocity distribution function due to the strong ECH theory. (Velocity space at the plug.)

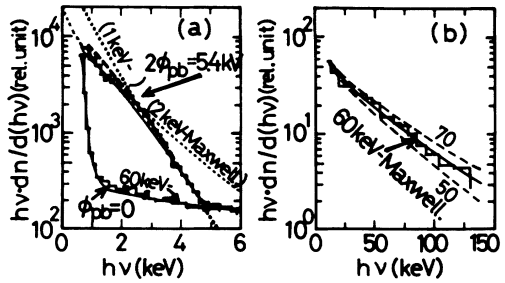

FIG. 2. (a) X-ray spectra for $2\phi_{pb}$=5.4 kV and 0. Data are fitted by plateau electron distribution functions (the maximum energy of 5.4 keV on axis) and with the ϕ_{pb} profile in Fig. 3(a) along with Maxwellian electrons (2.5% to the total n_p, 60 keV with a "loss-cone" angle of 35°) (the dashed curve). The contribution of the on-axis core electrons is shown by the solid curve. (b) The 60-keV Maxwellian electrons are observed. For comparison, x rays from Maxwellian electrons with 1 or 2 keV are shown by the dotted curves in (a).

Tandem Mirror Experiment TMX-U[13] as well as heavy-ion (Au^0) beam probes.[13,20]

In Fig. 1(a) the scaling data on ϕ_c vs ϕ_b are plotted with the ratio of the plug to the central-cell densities n_p/n_c=0.30–0.55 using ELA's (filled circles) and ELIS (open circles). The data are compared with the calculated results from the weak (dashed curves) and strong (solid curves) ECH theories. As compared with our previous results,[13] Fig. 1 clearly shows a transition from the weak, through the intermediate,[12] and then to the strong ECH prediction with increasing ϕ_b. From these ECH theories, this transition is expected to be accompanied by a change in f_{ep} from Maxwellian to the plateau distribution, since a remarkable thermal-isolation effect due to the ϕ_b increase causes an efficient heating of plug-localized electrons and thereby their drastically reduced collisions. Therefore, our next important issue is the observation of f_{ep} in this high-ϕ_b region. The axial configuration of ϕ_b, ϕ_c, and ϕ_{pb} is depicted in Fig. 1(b). In Fig. 1(c) a schematic drawing of f_{ep} resulting from the strong ECH theory is shown.[11] This velocity space is divided into three regions: The ϕ_{pb}-trapped electrons are confined in the regime P, where the plateau electrons are bounded by an ellipsoidal separatrix.[11] The Maxwellian electrons trapped by the plug and barrier mirror with a temperature T_{pm} are located in the region M; these electrons are heated by both plug and barrier ECH. The electrons in the region L are lost from the plug and barrier cell through the "loss cone" with an angle θ_0=35°.

The x-ray PHA data in the plug are represented with the Si(Li) detector [Fig. 2(a)]. The data are taken during PECH [potentials are formed as shown in Fig. 1(b)], as well as at 5 ms after PECH is switched off (ϕ_{pb} has already decayed to 0, but the other heating powers are still being injected). A remarkable feature is the quick decay of the x rays at $h\nu \leqq 5$ keV (in this case, $2\phi_{pb}$=5.4 kV) as compared with ϕ_{pb}=0. However, a higher-energy component, continued to at least 7 keV, does not change in either case. The data with the pure Ge detector are shown in Fig. 2(b) for the observation of such higher-energy x rays ($h\nu \geqq 5$ keV). Almost the same spectra in each case of ϕ_{pb} are again obtained (for simplicity, a spectrum for $2\phi_{pb}$=5.4 kV alone is represented there). Also, these spectra from the high-energy electron component observed with both detectors consistently show the same electron temperature of 60 keV.

For the x-ray spectrum analyses, the relativistic Born approximation[21,22] corrected by the Elwert factor[23] is used for the values of the x-ray cross section.[8] The x rays emitted at the detector angle[21] are calculated using various plateau distribution functions depending on ϕ_{pb} [see Fig. 1(c)] as well as relativistic Maxwellians[8] with various T_{pm} and θ_0. Impurity line radiation from both K and L shells[24] is not observed in Fig. 2(a); hence, impurities in the plasmas are ignored for the analyses (for more detail see Ref. 15).

X-ray observations with an NaI(Tl) detector in the barrier region[8] show an electron temperature of 60 keV as comparable to T_{pm}. These 60-keV electrons observed in both barrier and plug regions support the existence of the plug and barrier mirror-trapped electrons as predicted in the region M [Fig. 1(c)]. Even after the ϕ_{pb} decay, such mirror-trapped high-energy electrons are maintained as seen in Figs. 2(a) and 2(b), because of their low collisionality.

On the other hand, intense x rays from the lower-energy component below 5 keV are observed only when ϕ_{pb} is formed [Fig. 2(a)]. The spectrum is fitted using the calculated results from relativistic Maxwellian distributions; however, the dotted curves with 2 and 1 keV can fit the data ranging up to 2.5 keV alone, and exceeding 2.5 keV alone, respectively. No Maxwellian combinations can ever fit the spectrum with $\kappa = d\ln(h\nu dn)/d(h\nu)^2 < 0$, since Maxwellian electrons always emit photon spectra with $\kappa > 0$ as seen by these dotted curves. Such a spectrum with $\kappa < 0$ is one of the remarkable x-

ray characteristics from plateau electron distribution functions. The solid curve shown in Fig. 2(a) is calculated using f_{ep} in Fig. 1(c); here, we use the data of $2\phi_{pb}=5.4$ kV for the potential-trapped plateau electrons along with the mirror-trapped Maxwellian with a 35° loss cone ($T_{pm}=60$ keV and 2.5% to the total n_p). (The intensity of electron-electron bremsstrahlung is weaker by 2 orders of magnitude.) This fitting is based on the fact that dominant x rays come from hot core plasmas. More detailed analyses taking account of $\phi_{pb}(r)$ are carried out using f_{ep} in Fig. 1(c): A line-integrated intensity at $h\nu$ with the x-ray PHA, $I_{XP}(h\nu)$, is written as $\int[n_e n_i Z^2](r) I_{XC}(h\nu,r)dr$; here, I_{XC} for $h\nu$ at r is calculated using the ϕ_{pb} profile in Fig. 3(a). The product of $n_e n_i Z^2$ at r is obtained from tomographic-reconstructed x-ray emissivity at r, $I_{XT}(r)$, which is corrected by the absorber transmissivity and the MCP response,[15-19] divided by $\int I_{XC}(h\nu,r)d(h\nu)$, since $I_{XC}(h\nu,r)$ is normalized for unit values of electron and ion densities, n_e, n_i, and an ion effective charge Z. Thus, $I_{XP}(h\nu)$ is described by

$$\int\left[\left(I_{XT}(r)\Big/\int I_{XC}(h\nu,r)d(h\nu)\right)I_{XC}(h\nu,r)\right]dr.$$

In Fig. 3, the data from x-ray tomography for $I_{XT}(r)$ and the data on $\phi_{pb}(r)$ for calculating $I_{XC}(h\nu,r)$, therefore, predict the spectrum of $I_{XP}(h\nu)$ [the dashed curve in Fig. 2(a)]. Good agreement between the data and the calculation in Fig. 2(a) indicates the validity of the strong ECH theory, which predicts the model in Fig. 1(c). Here, the individual values of n_e, n_i, and Z are not necessary for the above analyses, since they are replaced by the tomography data.

Another independent method of comparing the x-ray data with the calculated x rays from the plateau distributions requires the assumptions of a low-Z (or a radially uniform Z) condition and of a small contribution of high-energy electrons to the total x rays (thereby, $n_e=n_i$); these are satisfied as described above. Now, we can calculate the x-ray profiles with various thickness absorbers from

$$\int[n_e n_i Z^2](r) I_{XC}(h\nu,r)d(h\nu)$$

[solid curves in Fig. 3(c)]. Here, we use $\phi_{pb}(r)$ and the model in Fig. 1(c) as well as the n_e profile deduced from x-ray data with a 1.8-μm polypropylene absorber (sensitive to $n_e n_i Z^2$ but insensitive to $h\nu$; see Ref. 8). This profile is consistent with those with microwave interferometers in the barrier and the central cell mapped along magnetic lines of force to the plug. Good agreement between the x-ray profile data and the calculations in Fig. 3(c) again proves the validity of the strong ECH plateau-formation theory.

The final issue in investigating this model is whether these plateau electrons are isolated by the thermal barrier and trapped in the plug. In Fig. 4 the absorption characteristics of the central-cell x rays (filled circles) are compared with those of the plug x rays (open circles) at $r=0$ in Fig. 3(c). The central-cell data are fitted by the 0.15-keV Maxwellian bulk electrons (T_{ec}) along with high-energy electrons (4 keV and 5% to the total n_c). Here, the bulk electron collision time of 30 μs and no ECH power in the central cell may form this Maxwellian distribution. These 4-keV electrons are also detected with ELA's; they may be explained by ECH-driven loss electrons through the loss cone of the plug,[12] since they appear during the PECH injection period only.

Such a remarkable electron-energy difference between the two regions has shown the first demonstration of the thermal-isolation effect due to a 1-kV-range thermal barrier. Also, different shapes of distribution functions are separated by the thermal barrier, indicating the information on the isolation of the ϕ_{pb}-trapped plug electrons by ϕ_b.

Here, it is useful to evaluate a criterion of validity of the strong ECH theory: Its essential requirement is whether the field strength of the plug ECH is large

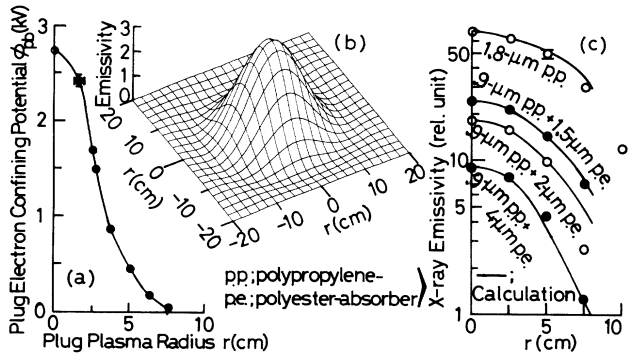

FIG. 3. (a) Radial profile data on ϕ_{pb}. (b) Tomographic-reconstructed x-ray emissivity using a 1.8-μm polypropylene absorber ($h\nu\geqq 80$ eV). (c) X-ray radial profile data with various absorbers are compared with the calculated x-ray profiles from the plateau electron distribution functions using the ϕ_{pb} data in (a).

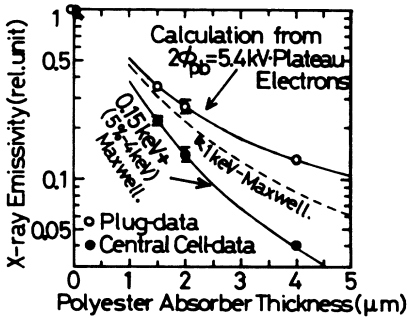

FIG. 4. X-ray tomography data ($r=0$) in the plug (○) (see Fig. 3) and in the central cell (●) are compared during the thermal-barrier period. Here, $h\nu\geqq 80$ eV.

enough to dominate over the plug-electron collisionality. Cohen has derived the equation for its criterion [see Eq. (9) in Ref. 11]. Using the plasma parameters ($n_p = 4 \times 10^{11}$ cm^{-3} and $T_{ec} = 150$ eV) and the GAMMA 10 machine parameters[13] (the axial scale length of B and the width of the plug region being 0.4 and 0.9 m, respectively), we obtain the critical field strength of 54 V cm^{-1}. The incident power of 100 kW forms the kV range of ϕ_c; this corresponds to the field intensity of a few hundred V cm^{-1}. This estimated value as well as a stronger BECH field producing 60-keV electrons may satisfy the strong ECH conditions.[11]

In summary, the first observation of a plateau-shaped plug electron distribution function for the potential-(ϕ_{pb}-) trapped electron-energy regime has been obtained using the x-ray PHA and tomography data. Also, mirror-trapped hot electrons in the same energy level as the 60-keV barrier electrons have been observed. These data along with the scaling relation between ϕ_c and ϕ_b for a kV range have shown the validity of Cohen's strong ECH theory for the ion-confining potential enhancement. Furthermore, the first observation of the thermal-isolation effect due to the kV-range thermal barrier has been obtained along with the different shapes of the electron distribution functions in the thermally isolated regions separated by the thermal barrier.

The authors would like to thank the other members of the GAMMA 10 group as well as Professor S. Tanaka of Kyoto University and Dr. T. Kato of Nagoya University for their useful discussions.

---

[a]Permanent address: Department of Energy System, Niigata University, Niigata, Japan.

[b]Permanent address: Japan Atomic Energy Research Institute, Naka-machi, Japan.

[c]Permanent address: Nagoya University, Nagoya, Japan.

[1]R. M. Gilgenbach *et al.*, Phys. Rev. Lett. **44**, 647 (1980).

[2]A. C. England *et al.*, Nucl. Fusion **29**, 1527 (1989).

[3]T. Cho and S. Tanaka, Phys. Rev. Lett. **45**, 1403 (1980).

[4]T. Cho *et al.*, Nucl. Fusion **26**, 349 (1986).

[5]A. Ando *et al.*, Phys. Rev. Lett. **56**, 2180 (1986).

[6]R. Prater, Bull. Am. Phys. Soc. **32**, 1712 (1987).

[7]R. F. Post, Nucl. Fusion **27**, 1579 (1987).

[8]T. Cho *et al.*, Nucl. Fusion **27**, 1421 (1987).

[9]N. Hershkowitz *et al.*, Nucl. Fusion **28**, 1333 (1988).

[10]R. H. Cohen *et al.*, Nucl. Fusion **20**, 1421 (1980); **23**, 1301 (1983).

[11]R. H. Cohen, Phys. Fluids **26**, 2774 (1983).

[12]R. H. Cohen and L. L. LoDestro, in *Physics of Mirrors, Reversed Field Pinches and Compact Tori,* Proceedings of the International School of Plasma Physics, edited by S. Ortolani and E. Sindoni (Società Italiana di Fisica, Bologna, 1987), Vol. II, p. 1187.

[13]T. Cho *et al.*, Nucl. Fusion **28**, 2187 (1988).

[14]T. Cho *et al.*, in *Proceedings of the Eleventh International Conference on Plasma Physics and Controlled Nuclear Fusion Research, Kyoto, Japan, 1986,* edited by J. W. Weil and M. Demir (IAEA, Vienna, 1987), Vol. 2, p. 243.

[15]T. Kondoh, T. Cho, M. Hirata, N. Yamaguchi, T. Saito, Y. Kiwamoto, and S. Miyoshi, J. Appl. Phys. (to be published).

[16]T. Kondoh *et al.*, Rev. Sci. Instrum. **59**, 252 (1988).

[17]T. Cho *et al.*, Rev. Sci. Instrum. **59**, 2453 (1988); **60**, 2337 (1989).

[18]N. Yamaguchi *et al.*, Rev. Sci. Instrum. **60**, 368 (1989); **60**, 2307 (1989).

[19]M. Hirata *et al.* (to be published).

[20]K. Ishii *et al.*, Rev. Sci. Instrum. **56**, 1053 (1985).

[21]R. L. Gluckstern *et al.*, Phys. Rev. **90**, 1026 (1953); **90**, 1030 (1953).

[22]A. C. England *et al.*, Phys. Rev. A **7**, 383 (1973); **8**, 1475 (1973).

[23]G. Elwert, Ann. Phys. **34**, 178 (1939).

[24]K. Masai *et al.*, Nature (London) **330**, 235 (1987); **335**, 804 (1988).